

# Site percolation on planar $\Phi^3$ random graphs

J-P. Kownacki\*

*Laboratoire de Physique Théorique et Modélisation  
CNRS-Université de Cergy-Pontoise - UMR8089*

*2, avenue Adolphe Chauvin, 95302 Cergy-Pontoise Cedex, France*

(Dated: August 27, 2021)

In this paper, site percolation on random  $\Phi^3$  planar graphs is studied by Monte-Carlo numerical techniques. The method consists in randomly removing a fraction  $q = 1 - p$  of vertices from graphs generated by Monte-Carlo simulations, where  $p$  is the occupation probability. The resulting graphs are made of clusters of occupied sites. By measuring several properties of their distribution, it is shown that percolation occurs for an occupation probability above a percolation threshold  $p_c=0.7360(5)$ . Moreover, critical exponents are compatible with those analytically known for bond percolation.

PACS numbers: 64.60.Ak, 04.60.Nc

## I. INTRODUCTION

Percolation on regular lattices has been extensively studied, both analytically and numerically [1]. It is now firmly established that critical exponents, governing scaling laws near percolation threshold, depend only on the dimension  $d$  of the lattice. On the contrary, percolation thresholds depend on the precise structure of the lattice. The complete knowledge of site and bond percolation thresholds for *all* regular lattices with given dimension is a very interesting challenge, from both theoretical and experimental points of view. It is also known that there exists an upper critical dimension  $d_c = 6$ . This means that for dimension  $d \geq d_c$ , all regular lattices belong to the same universality class as a family of regular lattices containing no loops, called Bethe lattices. This is due to the fact that the proportion of closed loops in a large regular lattice decreases with the dimension  $d$  and eventually becomes negligible for large  $d$ .

On the other hand, percolation on *random* graphs is still an open subject. One class of such random graphs, called complex networks, containing scale free networks and Erdős-Rényi networks, is at present attracting a lot of interest in physical and mathematical communities as they are good models for real networks (world wide web, social networks, ...) [2]. A crucial feature of complex networks is that closed loops can be neglected for large graphs. Percolation theory have been recently used to investigate their intrinsic properties [3].

A radically different family of random graphs have been extensively studied in the past decades as a non-perturbative regularization of quantum gravity (see [4] for a review). Contrary to complex networks, they are planar, with closed loops that cannot be neglected. Moreover, distant vertices are strongly correlated. In some sense, these graphs are closer to regular lattices than complex networks. More precisely, they look *locally* like a

regular lattice but are globally very different. This intermediate situation makes the problem of percolation on these graphs very exciting. Planar  $\Phi^3$  random graphs, or their dual planar dynamical triangulations, belong to this family. They are defined in section II of this paper. Their properties are rather well established now on the ground of a great amount of analytical and numerical results [5]. In particular, it is known that the Hausdorff dimension of these graphs is  $d_H = 4$  [6] with a fractal structure of so-called baby universes [7]. Percolation on planar  $\Phi^3$  random graphs is the subject of this paper. In fact, *bond* percolation on planar  $\Phi^3$  random graphs has been exactly solved as the limit  $q \rightarrow 1$  of a  $q$ -state Potts model, using matrix models [8]. In this article, we study numerically *site* percolation on these graphs. The main purpose is to measure the value of the percolation threshold. Moreover, our work is a test of universality between site and bond percolation for this model.

## II. THE MODEL

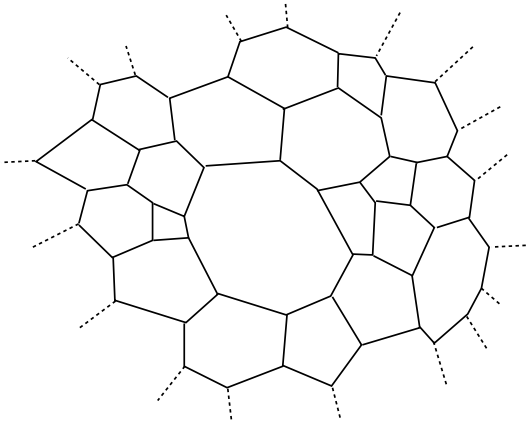
### A. Random $\Phi^3$ planar graphs

We consider the set of all planar graphs with  $N$  trivalent vertices, *i.e* graphs without boundaries that can be drawn on a sphere and where each vertex is linked to exactly three neighbors. Moreover, two distinct vertices can be linked by at most one link and no vertex can be linked to itself (see Fig. 1).

These graphs are purely topological objects as no length scale is given here. Such graphs are characterized by their Euler number  $\chi = N - N_l + N_f = 2$ , where  $N$ ,  $N_l$ , and  $N_f$  are respectively the number of vertices, links and faces. Moreover, local properties of these graphs imply  $2N_l = 3N$ . However, there is no constraint on the size of a face, *i.e* the number of links surrounding a face, except that it must be greater than three. Note that, in some cases (degenerate graphs), some loops contain almost all links of the graph. This set, called  $\Phi^3$  planar graphs, is turned into a statistical model by assigning a Boltzmann

---

\*Electronic address: kownacki@ptm.u-cergy.fr

Figure 1: A  $\Phi^3$  graph.

weight to each graph. In this paper, each graph has the same weight. The partition function of this ensemble of random graphs is written

$$Z_N = \sum_{G \in \Phi^3|_N} \frac{1}{C(G)}$$

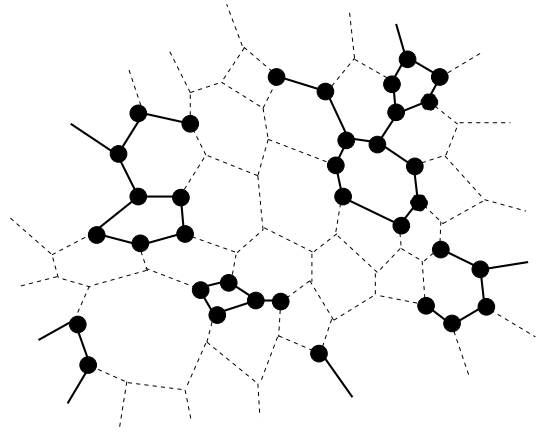
where the sum is over all  $\Phi^3$  graphs with  $N$  vertices as defined above, and  $C(G)$  is a symmetry factor which avoids the overcounting of some symmetric graphs ( $C(G)$  is almost always equal to one for large graphs). The size of each face can be seen as a random variable, with mean value equal to six, whose distribution can be exactly calculated [9]. However, topological constraints (planarity) imply strong correlations between distant faces. As an example, correlation between adjacent faces follow a modified Aboav's law [10]. Another important feature of these graphs is their Hausdorff dimension, which has been shown to be  $d_H = 4$  [6]. It can be defined as follows: first define a path between two vertices  $v_1$  and  $v_2$  as a succession of adjacent links connecting  $v_1$  and  $v_2$ . The length of the path is the number of links in the path and the geodesic distance between  $v_1$  and  $v_2$  is the length of the shortest path between them.  $\langle N_r \rangle_o$ , the mean number of vertices whose geodesic distance from an arbitrary vertex  $v_o$  is lower than  $r$ , scales (for large  $r$ ) as

$$\langle N_r \rangle_o \sim r^{d_H}$$

## B. Site percolation

### 1. Definition

We now consider the problem of site percolation on these graphs. As usual, each site (vertex) of a graph  $G$  is randomly occupied or empty, independently of the rest of the sites. More precisely, each site is occupied with probability  $p$  or empty with probability  $q = 1 - p$  (see Fig. 2). Each distribution of occupied and empty

Figure 2: Occupied (black bullets) and empty sites on a  $\Phi^3$  graph. Dashed links connect empty sites to occupied or empty sites.

sites on  $G$  induces a structure of clusters. A cluster is a set of occupied sites connected by links of  $G$ . The study of average properties of these clusters as  $p$  is varied is the subject of percolation theory. Consider a graph  $G \in \Phi^3|_N$  and a distribution of occupied/empty sites on  $G$ , denoted  $\mathcal{D}$  (for a given occupation probability  $p$ ); suppose that a quantity  $A = A[G, \mathcal{D}]$  depends on  $G$  and  $\mathcal{D}$ . The annealed average quantity  $\langle A \rangle(N, p)$  is obtained by first averaging on all distributions  $\mathcal{D}$  for a given graph  $G$  and, then, by averaging on all graphs  $G$ . It can be written:

$$\langle A \rangle(N, p) = \sum_{G \in \Phi^3|_N} \frac{1}{C(G)} \sum_{\mathcal{D}} A[G, \mathcal{D}]$$

$\langle A \rangle(N, p)$  can be seen as the (average) value of  $A$  on a graph picked at random from the  $\Phi^3|_N$  ensemble.

### 2. Cluster distribution

For fixed  $p$ , the distribution of the sizes of clusters is described by the quantity  $n(s, p)$ , equal to the density of clusters made of  $s$  connected sites. Alternatively, one is interested by all the moments of the distribution:  $K_n(p) = \sum'_s n(s, p) s^n$ , where the symbol  $\sum'$  means that only finite clusters enter the sums. In practice, only the first moments are usually studied. More precisely,  $K_o(p) = \sum'_s n(s, p)$  is the total number per site of finite clusters;  $K_1(p) = \sum'_s n(s, p) s$  is the probability that a site belongs to any finite cluster and  $S(p) = \sum'_s n(s, p) s^2 / \sum'_s n(s, p) s$  is one way to define the mean cluster size.

Other interesting quantities are  $s_1(p)$ ,  $s_2(p)$ , ..., defined as the sizes of the largest, second largest, ... cluster.

### 3. Percolation threshold

One of the most basic questions is the existence, in the thermodynamic limit  $N \rightarrow \infty$ , of a percolation threshold  $p_c$  such that, for  $p < p_c$ , all clusters have a finite size and, for  $p > p_c$ , there exists at least one spanning cluster. This is formally expressed by defining a probability  $R(p)$  that there exists a spanning cluster, with  $R(p) = 0$  for  $p < p_c$  and  $R(p) = 1$  for  $p > p_c$ . The definition of a spanning cluster is not unique but, practically, it can be seen as a cluster connecting two opposite boundaries on a lattice. Unfortunately, such a definition does not easily apply for the family of graphs considered in this paper, as there is no natural way to define opposite boundaries in these graphs. However, this can be circumvented by defining  $p_c$  as the value of  $p$  for which the sizes of the second, third, ... largest clusters reach a maximum [11]. This property can be understood with the following heuristic argument: for  $p < p_c$ , all graphs contain several finite clusters with comparable size, as soon as  $p$  is not too close to  $p_c$ . As  $p$  is growing, the sizes of the largest, second largest, third largest ... clusters are growing until  $p_c$  is reached. At this point, most of the clusters merge into a giant component so that, for  $p > p_c$ , the sizes of the second, third, ... largest clusters dramatically fall down.

### 4. Critical exponents

There is a profound analogy between percolation and critical phenomena, where  $p_c$  plays the role of the critical temperature. The analog of the order parameter is the density of the spanning cluster, denoted  $\mathcal{P}(p)$ . It represents the probability for a site to belong to the spanning cluster. It can be defined as  $\mathcal{P}(p) = p - \sum_s' n(s, p) s$  since  $p$  is the probability for a site to belong to a cluster (finite or not) and  $\sum_s' n(s, p) s$  is the probability for a site to belong to a finite cluster. For  $p < p_c$ , all clusters are finite and  $\mathcal{P}(p) = 0$ . For  $p > p_c$ ,  $\mathcal{P}(p)$  increases with  $p$  and  $0 < \mathcal{P}(p) \leq 1$ . However, for planar  $\Phi^3$  random graphs, the notion of spanning cluster is not appropriate, and  $\mathcal{P}(p)$  is defined as the density of the largest cluster. At least for  $p \sim p_c$  and large graphs, both definitions are expected to coincide.

As in critical phenomena, it is possible to define a correlation length  $\xi(p)$  related to the mean radius of clusters and diverging at  $p = p_c$  as  $\xi(p) \sim (p - p_c)^{-\nu}$ . Moreover, most observables are expected to follow scaling laws in the region  $p \sim p_c$ . We define standard exponents  $\alpha, \beta$  and  $\gamma$  associated with  $K_o(p)$ ,  $\mathcal{P}(p)$ ,  $S(p)$  in the critical region by

$$\begin{aligned} K_o(p) &\sim (p - p_c)^{2-\alpha} \\ \mathcal{P}(p) &\sim (p - p_c)^\beta \\ S(p) &\sim (p - p_c)^{-\gamma} \end{aligned}$$

and, at  $p = p_c$ ,  $n(s) = n(s, p_c)$  is expected to scale

with an exponent  $\tau$  as

$$n(s) \sim s^{-\tau}$$

These exponents are expected to follow the scaling relations

$$\begin{aligned} 2 - \alpha &= \gamma + 2\beta = d\nu \\ \tau &= 2 + \frac{\beta}{d\nu - \beta} \end{aligned} \quad (1)$$

Here,  $d$  is a parameter characteristic of the model. For regular  $D$ -dimensional lattices with  $D \leq 6$ ,  $d = D$  is the standard dimension of the lattice. For  $D \geq 6$ , i.e. above the upper critical dimension,  $d = 6$ . For planar  $\Phi^3$  random graphs,  $d = d_H = 4$ , the Hausdorff dimension defined above.

The sizes of the largest, second largest, ... clusters follow a scaling law [11]

$$\begin{aligned} s_1 &\sim (p - p_c)^{\beta - \nu d} \\ s_2 &\sim (p - p_c)^{\beta - \nu d} \\ &\vdots \end{aligned}$$

### 5. Theoretical values of critical exponents for bond percolation

Percolation could be defined by an occupation probability on the links of the planar  $\Phi^3$  random graphs. This would give rise to *bond percolation*. As in critical phenomena, critical exponents are expected to be universal whereas  $p_c$  should depend on the details of the model. So, critical exponents should be the same in bond and site percolation. Bond percolation on planar  $\Phi^3$  random graphs has been exactly solved using a random matrix model formulation [8], so that exponents  $\nu, \alpha, \beta, \gamma$  and  $\tau$  are exactly known in this case [12]:

$$\nu = 1, \quad \alpha = -2, \quad \beta = \frac{1}{2}, \quad \gamma = 3, \quad \tau = \frac{15}{7}$$

If universality holds, critical exponents for site percolation should also be given by these values.

## III. THE NUMERICAL EXPERIMENT

### A. The method

#### 1. Nodes removal

The first coincidence is to generate graphs in  $\Phi^3|_N$ . We start from a tetrahedron. Then, one face (triangle) is randomly chosen, a vertex is added inside this face and linked to the three vertices of the triangle. This procedure is repeated until a polyhedron with  $N$  faces (triangles) is obtained. This polyhedron is transformed

into a  $\Phi^3$  graph by duality, *i.e.* each face (triangle) of the polyhedron is replaced by a vertex linked to three vertices associated to the three adjacent faces of the triangle. The graph  $G^{(o)}$  thus obtained contains  $N$  trivalent vertices and has the topology of a sphere. Then, starting from  $G^{(o)}$ , all graphs in  $\Phi^3|_N$  can be generated by using standard flips of links called  $T_2$  moves [4].

Once a graph  $G \in \Phi^3|_N$  has been obtained, one distribution  $\mathcal{D}(G, p)$  of occupied and empty sites is randomly generated. This is achieved by randomly removing  $qN$  vertices from  $G$ , with  $q = 1 - p$ . The  $pN$  remaining vertices are defined as occupied vertices on  $G$ . Then, interesting quantities are measured. Several distributions are generated this way to obtain average properties on  $G$  for fixed  $p$ . Then, another graph is generated by a serie of  $T_2$  moves and the removal procedure is applied to this new graph, *etc.* Annealed averages of observables are thus computed.

## 2. Cluster construction and measured quantities

For each distribution  $\mathcal{D}(G, p)$  on a given graph  $G$ , all clusters are constructed using a breadth-first search algorithm analog to Wolff algorithm [13]. At step  $n - 1$  of the algorithm, suppose  $n - 1$  clusters  $c_1, c_2, \dots, c_{n-1}$  have already been constructed. All corresponding occupied sites are labeled “visited”. Step  $n$  first consists in choosing an occupied site not yet visited. This site  $v_o$  is the root of the cluster  $c_n$  and is now labeled “visited”. It is put in a (empty) list  $Q$ . The following procedure is now applied to  $Q$ : for each site  $v$  in  $Q$ , all occupied and not yet visited neighbors of  $v$  on  $G$  are added to  $c_n$ , labeled “visited” and put in  $Q$  whereas  $v$  is removed from  $Q$ . This procedure is repeated until  $Q$  becomes empty. The cluster  $c_n$  is thus completely constructed. The algorithm stops when all occupied vertices have been visited.

The size of each cluster - *i.e.* the number of sites in the cluster - is registered and a histogram of the sizes is built. This allows to measure the following quantities:

- $K_o(p)$ , the total number of clusters (except the largest one);
- $n(s, p)$ , the density of clusters of size  $s$ ;
- $\mathcal{P}(p)$ , the size of the largest cluster divided by  $N$ ; for large  $N$ , this is expected to represent the order parameter defined above;
- $s_2(p)$ , the size of the second largest cluster ;
- $K_2(p)$ , the second moment of  $n(s, p)$ ; in the critical region,  $K_2(p)$  is expected to scale like  $S(p) = K_2(p)/K_1(p)$ , the mean (finite) cluster size .

## 3. Finite size scaling

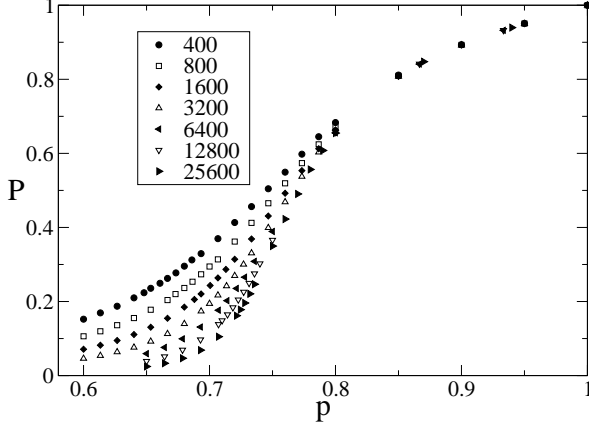
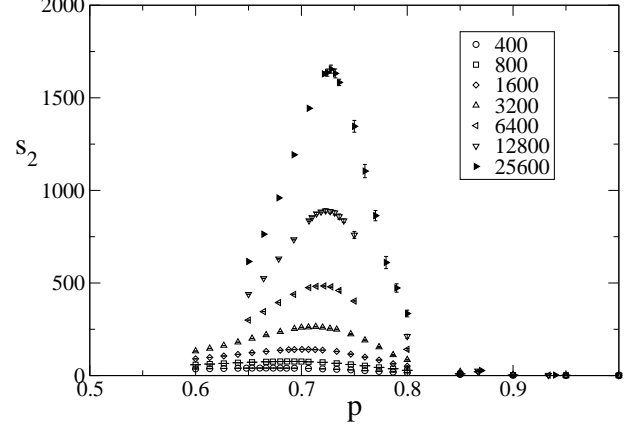
An important tool when using numerical simulations is the finite size scaling analysis. It is based on the hypothesis that, for finite systems, scaling laws are corrected by scaling functions depending on the ratio between the linear size  $L$  of the system and the correlation length  $\xi$ . More precisely, for  $L \gg \xi$ , the system should not feel finite size effects, but when the correlation length becomes of order  $L$ , finite size should modify scaling laws. For a quantity  $O$ , a scaling law  $O \sim (p - p_c)^{-z}$  (for infinite size of the system) can be rewritten  $O \sim \xi^{z/\nu}$  as the correlation length itself scales as  $\xi \sim (p - p_c)^{-\nu}$ . Then, when  $\xi \sim L$ ,  $O \sim L^{z/\nu}$ . This can be summarized by  $O \sim L^{z/\nu} F((p - p_c) L^{1/\nu})$  where  $F(x)$  is a (scaling) fonction of the dimensionless ratio  $x = (p - p_c) L^{1/\nu} \sim (L/\xi)^{1/\nu}$  such that  $F(x) \rightarrow 1$  for  $x \sim 1$  and  $F(x) \rightarrow x^{-z}$  for  $x \gg 1$ .

Finite size scaling laws enable one to extract the values of critical exponents by studying the behavior of quantities as the size of the system is varied. This also defines a finite size percolation threshold: suppose that the scaling function for  $O$  reaches a maximum for  $x = x_o$ . Then, for fixed  $L$ , the value of  $p$  for which  $O$  reaches a maximum is given by  $(p - p_c) L^{1/\nu} = x_o$ . This defines an effective finite size percolation threshold  $p_c(L)$  approaching  $p_c$  when  $L \rightarrow \infty$  as  $p_c(L) - p_c \sim L^{-1/\nu}$  [1].

For percolation on graphs in  $\Phi^3|_N$ , there is no explicit linear size as graphs are purely topological. However, the quantity  $N^{1/d_H}$ , where  $d_H$  is the Hausdorff dimension, defines an effective linear size, so that finite size scaling can be written  $O \sim L^{z/\nu} F((p - p_c) N^{1/\nu d_H})$ . The effective finite size percolation threshold  $p_c(N)$  then approaches  $p_c$  as  $p_c(N) - p_c \sim N^{-1/\nu d_H}$ .

## B. Simulations

We simulated graphs of sizes ranging from  $N = 400$  to  $N = 25600$  or  $N = 51200$  (according to the measured quantity) vertices. When measuring  $\mathcal{P}(p)$  and  $s_2(p)$ , we considered various values of  $p$  for each size. For each graph  $G$  and given  $p$ , we generated  $n_D = 128$  to 1024 occupation distributions by the nodes removal method.  $n_D$  was chosen big enough to minimize its influence on annealed averages. Each simulation consisted in generating  $n_G$  graphs in  $\Phi^3|_N$ , with  $n_G$  ranging from 1024 to 4096 for each value of  $p$ . Each graph was obtained from the previous one by performing 2000  $N_l$  flips ( $T_2$  moves). We estimated error bars by standard jackknife method. Error bars are always plotted on the figures below but, most of the time, they are hidden by the symbols.

Figure 3: Order parameter  $\mathcal{P}$  vs  $p$ .Figure 4: Size of the second largest cluster  $s_2$  vs  $p$ .

### C. The results

#### 1. Order parameter

The percolation order parameter  $\mathcal{P}$  plotted as a function of  $p$  is shown in Fig. 3, for various values of  $N$ . We see that, for low values of occupation probability  $p$ ,  $\mathcal{P}$  is close to zero. As expected,  $\mathcal{P} = 1$  for  $p = 1$  since all graphs are connected when no vertex is removed. According to percolation theory,  $\mathcal{P}$  is not zero only in the percolating phase. As can be seen on the figure, in our model, a percolation transition is expected to take place for  $p \simeq 0.7$ . However, it is not possible to get a precise estimate of the threshold value  $p_c$  with these data.

#### 2. Percolation threshold $p_c$

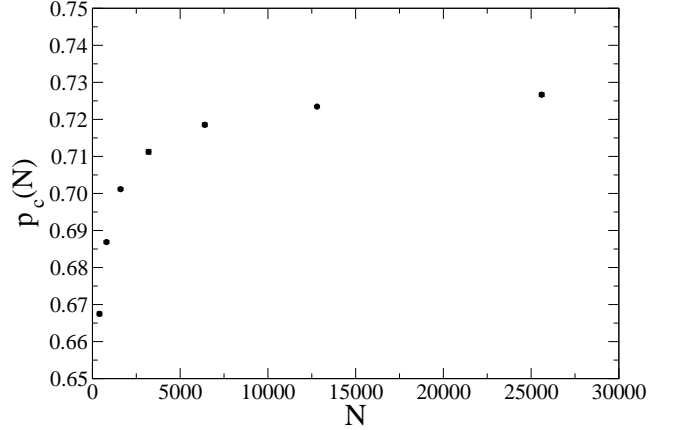
The percolation threshold  $p_c$  is determined using the behavior of  $s_2$ , the size of the second largest cluster. Fig. 4 clearly shows a peak of  $s_2$  for a value depending on  $N$ , denoted  $p_c(N)$ . This effective percolation threshold  $p_c(N)$  was extracted by fitting the peaks of  $s_2$  with quadratic functions. The result is plotted in Fig. 5. As explained above, by using finite size scaling hypothesis,  $p_c(N)$  is expected to approach  $p_c$  for large  $N$  according to

$$p_c(N) = p_c + c_1 N^{-1/\nu d_H} \quad (2)$$

where  $c_1$  is a constant. So, we fitted  $p_c(N)$  with the scaling law (2) and we obtained  $p_c = 0.7360(5)$ .

#### 3. Critical exponents

· Exponent  $\nu$ .

Figure 5: Finite size percolation threshold vs  $N$ .

The fit of  $p_c(N)$  with the scaling law (2) allowed us to extract also the value of  $1/\nu d_H$ . We obtained  $1/\nu d_H = 0.489(9)$ . As can be seen in Fig. 6,  $p_c(N)$  is clearly a straight line when plotted as a function of  $N^{-0.489}$ .

· Exponent  $\beta$ .

We also used  $s_2$  to extract  $\beta/\nu d_H$ : Fig. 4 shows that the peaks of  $s_2$  are growing with the size  $N$ . By fitting the peaks of  $s_2$  with quadratic functions, we obtained the value of  $s_2$  at the maximum, denoted at  $s_2^{max}(N)$ . Fig. 7 shows the results.

By finite size scaling arguments,  $s_2$  is expected to behave as

$$s_2 \sim N^{1-\beta/\nu d_H} F\left((p - p_c) N^{1/\nu d_H}\right)$$

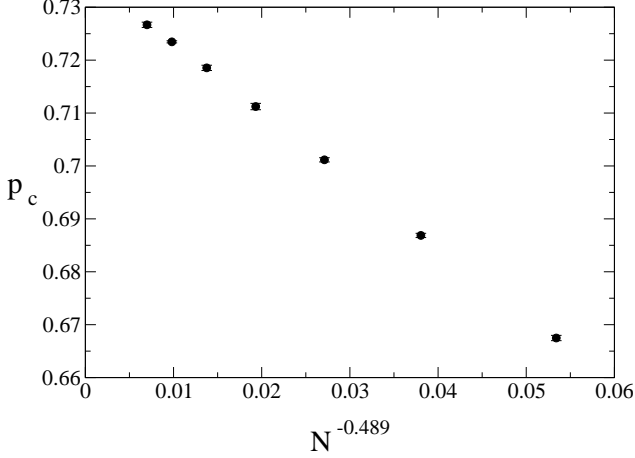


Figure 6: Finite size percolation threshold plotted as a function of  $N^{-0.489}$ .

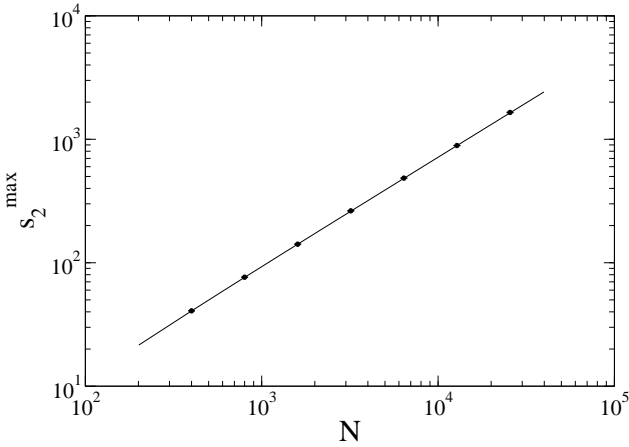


Figure 7: Maximum of  $s_2$  vs  $N$ . The straight line is the best fit.

so that  $s_2^{max}(N)$  scales as

$$s_2^{max} \sim N^{1-\beta/\nu d_H} \quad (3)$$

By fitting  $s_2^{max}(N)$  with the scaling form (3), we obtained  $1 - \beta/\nu d_H = 0.880(1)$ . The best fit is plotted in Fig. 7.

· exponent  $\tau$

We measured the number of clusters of size  $s$  at  $p = p_c = 0.7360$ . In order to extract the value of  $\tau$ , we did not use finite size scaling analysis. Instead, we used the scaling law (for  $s \gg 1$ )

$$n(s) \sim s^{-\tau} \quad (4)$$

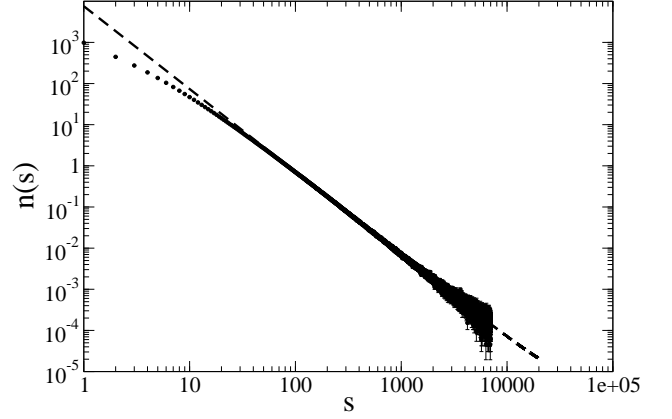


Figure 8: Number of clusters of size  $s$  (not normalized) for  $p = p_c$  and  $N = 51200$ . The straight line is the best fit.

for one value of  $N$  large enough to minimize finite size effects. We chose  $N = 51200$  and discarded data with  $s \gtrsim 100$  and  $s \lesssim 7000$  (because the scaling form is valid for  $s \gg 1$  and there was not enough statistic beyond  $s = 7000$ ). Then, we fitted the data with the scaling form (4). We obtained  $\tau = 2.0(1)$ . The result is shown in Fig.8.

· Exponent  $\alpha$

We extracted the value of  $\alpha$  by using finite size scaling analysis applied to the density of total number of clusters  $K_o(p)$  measured at  $p = p_c$  (Fig. 9). The expected scaling law is

$$K_o(N, p_c) \sim N^{(\alpha-2)/\nu d_H} \quad (5)$$

We fitted data with (5) and obtained  $(\alpha - 2)/\nu d_H = -0.7(2)$ . The result is plotted in Fig. 9

· Exponent  $\gamma$

We measured  $K_2(p)$ , the second moment of the distribution  $n(s, p)$  for  $p = p_c$ . Fig. 10 shows the result. As mentioned above,  $K_2(p)$  is expected to scale as  $S(p)$ , the mean size of finite clusters, at least in the critical region. Finite size scaling law for  $K_2(p)$  is then

$$K_2(N, p_c) \sim N^{\gamma/\nu d_H} \quad (6)$$

We extracted  $\gamma$  by fitting data with (6) and we obtained  $\gamma/\nu d_H = 0.67(3)$

#### 4. Remark on the results

The determination of the percolation threshold using the maximum of the second largest cluster gives rather

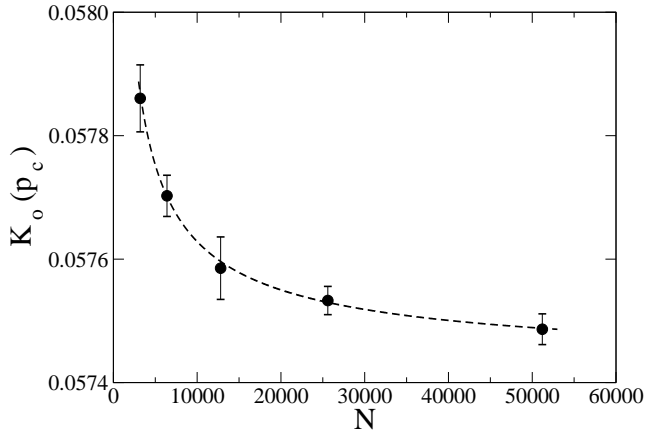


Figure 9: Density of total number of cluster measured at  $p = p_c$ . The dashed curve is the the best fit.

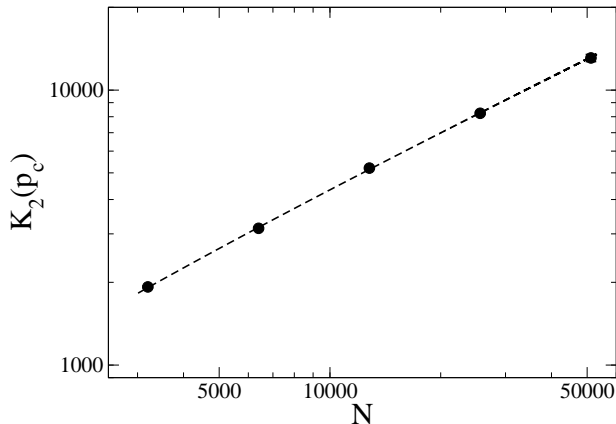


Figure 10: Second moment of  $n(s, p)$  for  $p = p_c$ . The dashed line is the best fit.

accurate value for  $p_c$ . This is partly due to the fact that the parameter  $p_c$  in the scaling law (2) is independent of the precise approach of  $p_c(N)$  to its infinite size limit.

The situation is rather different for the determination of critical exponents. In Table II, measured and theoretical values of critical exponents considered in this paper are summarized. In addition, combinations entering scaling relations (1) are given in Table III. As can be seen, the value of  $1/\nu d_H$  obtained by simulations is not compatible with the theoretical value  $1/4$ . In fact, it is well known that the Hausdorff dimension of planar  $\Phi^3$  random graphs is very sensitive to finite size effects and can be extracted only for large lattices using sophisticated scaling variables in finite size scaling analysis [14]. However, this does not mean that simulations are unable to take

Exponent	$1/\nu d_H$	$(\alpha - 2)/\nu d_H$	$\beta/\nu d_H$	$\gamma/\nu d_H$	$\tau$
Simulation	0.489(9)	-0.7(2)	0.120(1)	0.67(3)	2.0(1)
Theory	0.25	-1	0.125	0.75	15/7

Table II: Theoretical and measured values of critical exponents.

Combination	$(\gamma + 2\beta)/\nu d_H$	$2 + \frac{\beta/\nu d_H}{1 - \beta/\nu d_H}$
Simulation	0.91(3)	2.136(1)
Theory	1	$\frac{15}{7}$

Table III: Test of scaling relations between critical exponents

account of the fractal structure of these graphs. The remaining critical exponents are compatible ( $\beta/\nu d_H, \tau$ ) or marginally compatible ( $(\alpha - 2)/\nu d_H, \gamma/\nu d_H$ ) with the theoretical values. However, error bars take into account neither the error on  $1/\nu d_H$  nor the uncertainty in determining  $p_c$ . Moreover, logarithmic corrections to scaling should be considered to obtain accurate values of the exponents.

#### IV. CONCLUSION

The first important fact is to notice that critical exponents and scaling relations obtained by simulations are globally compatible with the expected theoretical values calculated for bond percolation. This gives confidence in the extraction of the (unknown) site percolation threshold. This also confirms universality between site and bond percolation for this model.

However, the main result of this paper is the value  $p_c = 0.7360(5)$  for site percolation on planar  $\Phi^3$  random graphs. It is greater but not very far from the threshold value for site percolation on the honeycomb lattice  $p_c(\text{honeycomb}) = 0.6962\dots$ , which is the simplest regular trivalent lattice. On one hand, this means that, to some extent, planar  $\Phi^3$  random graphs and honeycomb lattices look alike: more precisely, they *locally* look alike. In contrast, trivalent Bethe lattices are neither locally equivalent to honeycomb nor to planar  $\Phi^3$  random graphs, so that their percolation thresholds are very different,  $p_c(3 - \text{Bethe lattice}) = 1/2$ . On the other hand, as  $p_c$  is greater for planar  $\Phi^3$  random graphs than honeycomb lattices, percolation is easier on a pure hexagonal lattice than on the planar  $\Phi^3$  random graphs. The reason is that on these latter graphs, there are regions called baby universes (B.U.) connected to the rest of the graph by very small boundaries called necks [7]. Moreover, B.U. can grow on other B.U., giving a fractal (self-similar) structure to the graph. So, for a given occupation probability  $p$ , the probability that a given B.U. belongs to a giant connected cluster is proportional to the probability that at least one vertex of its boundaries is occupied. This is small compared with the probability that, on a pure hon-

eycomb lattice, a given region is a part of a giant cluster. This fractal structure of B.U. is also the main feature that makes honeycomb lattice and planar  $\Phi^3$  random graphs globally different at long distance, so that their critical exponent are different.

It would be interesting to study in more details the connections between baby universes and percolation transition. In particular, a non-uniform occupation probability, depending for instance on the local curvature or on the structure of B.U., could shed light on this problem. The role of B.U. could also be studied by real-space renormalization group analysis. As mentioned above, planar  $\Phi^3$  random graphs have a hierarchical structure that makes them look like trees of baby universes. It is possible to use this self-similarity of planar  $\Phi^3$  ran-

dom graphs with respect to B.U. to perform a real-space renormalization group transformation [15] by replacing each baby universe of last generation (*i.e.* a B.U. with no further B.U. growing on it) by one supersite [1]. Then, if the corresponding last generation B.U. (including its boundary) contained a spanning cluster, the supersite is occupied. This defines an occupation probability  $p'$  for the supersite as a (complicated) function of  $p$ , the occupation probability of the original graph.

It should also be noticed that the value of  $p_c$  found here is comparable with high values found on Archimedean lattices [16]. It would be interesting to understand if planar  $\Phi^3$  random graphs share common *local* characteristics with Archimedean lattices.

- 
- [1] D. Stauffer and A. Aharony, *Introduction to percolation theory*, Taylor & Francis, New-York, (1994); D. Stauffer, *arXiv:07043848*.
  - [2] R. Albert and A.-L. Barabasi, *Rev. Mod. Phys.* **74**, 47 (2002); S.N. Dorogovtsev, A.V. Goltsev and J.F.F. Mendes, *arXiv:0705.0010*.
  - [3] D.S. Callaway, M.E.J. Newman, S. H. Strogatz and D. J. Watts, *Phys. Rev. Lett.* **85**, 5468 (2000); R. Cohen, D. ben-Avraham and S. Havlin, *Phys. Rev. E* **66**, 036113 (2002); Z. Wu, C. Lagorio, L.A. Braunstein, R. Cohen, S. Havlin and H.E. Stanley, *Phys. Rev. E* **75**, 066110 (2007); J.D. Noh, *Phys. Rev. E* **76**, 026116 (2007); H.D. Rozenfeld and D. ben-Avraham, *Phys. Rev. E* **75**, 061102 (2007).
  - [4] F. David, in *Gravitation and Quantizations*, Les Houches Session LVII (1992); J. Ambjørn, in *Fluctuating Geometries and Field Theory*, Les Houches Session LXII (1994); P. Di Francesco, P. Ginsparg and J. Zinn-Justin, *Phys. Rep.* **254**, 1 (1995); J. Ambjørn, B. Durhuus, and T. Jonsson, *Quantum Geometry*, Cambridge University Press, (1997).
  - [5] M. Weigel and D. Johnston, *Phys. Rev. B* **76**, 054408 (2007).
  - [6] H. Kawai, N. Kawamoto, T. Mogami and Y. Watabiki, *Phys. Lett. B* **306**, 19 (1993); J. Ambjørn and Y. Watabiki, *Nucl. Phys. B* **445**, 129 (1995).
  - [7] S. Jain and S.D. Mathur, *Phys. Lett. B* **286**, 239 (1992).
  - [8] V.A. Kazakov, *Nucl. Phys. B (Proc. Supp.)* **4**, 93 (1988); V.A. Kazakov, *Mod. Phys. Lett. A* **4**, 1691 (1989).
  - [9] D.V. Boulatov, V.A. Kazakov, I.K. Kostov and A.A. Migdal, *Nucl. Phys. B* **275**, 641 (1986).
  - [10] C. Godreche, I. Kostov and I. Yekutieli, *Phys. Rev. Lett.* **69**, 2674 (1992).
  - [11] A. Margolina, H.J. Herrmann and D. Stauffer, *Phys. Lett. A* **93**, 73 (1982).
  - [12] G. Harris, *Nucl. Phys. B* **418**, 278 (1994).
  - [13] U. Wolff, *Phys. Rev. Lett.* **62**, 361 (1989).
  - [14] M.E. Agishtein and A.A. Migdal, *Nucl. Phys. B* **350**, 690 (1991); M.E. Agishtein and A.A. Migdal, *Int. J. Mod. Phys. C* **1**, 165 (1990); M.E. Agishtein, L. Jacobs and A.A. Migdal, *Mod. Phys. Lett. A* **5**, 965 (1990); M.E. Agishtein, R. Ben-Av, A.A. Migdal and S. Solomon, *Mod. Phys. Lett. A* **6**, 1115 (1991); S. Catterall, G. Thorleifsson, M. Bowick and V. John, *Phys. Lett. B* **354**, 58 (1995).
  - [15] D.A. Johnston, J.-P. Kownacki and A. Krzywicki, *Nucl. Phys. B (Proc. Supp.)* **42**, 728 (1995); Z. Burda, J.-P. Kownacki and A. Krzywicki, *Phys. Lett. B* **356**, 466 (1995).
  - [16] P. N. Suding and R. M. Ziff, *Phys. Rev. E* **60**, 275 (1999); C. R. Scullard and R. M. Ziff, *Phys. Rev. E* **73**, 045102(R) (2006).